applied sciences

MDPI

Article

Adsorption of Ibuprofen from Water Using Waste from Rose Geranium (*Pelargonium graveolens*) Stems

Ntaote David Shooto * and Patience Mapule Thabede

Natural Sciences Department, Vaal University of Technology, P.O. Box X021, Vanderbijlpark 1900, South Africa; patiencet@vut.ac.za

* Correspondence: ntaotes@vut.ac.za

Abstract

Rose geranium is widely used for oil extraction and in the food, perfume, and pharmaceutical industries. The waste produced after oil extraction has no alternative use and is usually dumped into the environment, causing pollution. This study aimed to use waste rose geranium stems (SPG) as a potential adsorbent for ibuprofen from water. The adsorbent was characterised by SEM-EDX, FTIR, TGA, and BET. The SEM images showed that the adsorbent had a rough surface with voids and pores. Different functional groups were detected on the surface of SPG with FTIR. The trend of IBU adsorption showed that the adsorption capacity increases when the initial concentration of working standards is increased. The data for the contact time effect show that the adsorption rate was fast in the initial stage between 1 and 45 min. Afterward, a slow adsorption rate occurred between 65 and 105 min. The kinetic data corresponded to the Langmuir and pseudo-first-order (PFO) models. The highest recorded IBU uptake was 34.88 mg/g. The ΔH^o value shows that the adsorption of IBU on SPG was controlled by physisorption. The obtained values of ΔG^o are negative, indicating that the uptake of IBU was spontaneous.

Keywords: adsorption; ibuprofen; *Pelargonium graveolens*; stem

check for updates

Academic Editor: Juan García Rodríguez

Received: 17 March 2025
Revised: 4 June 2025
Accepted: 6 June 2025
Published: 26 June 2025

Citation: Shooto, N.D.; Thabede, P.M. Adsorption of Ibuprofen from Water Using Waste from Rose Geranium (*Pelargonium graveolens*) Stems. *Appl. Sci.* **2025**, *15*, 7203. https://doi.org/10.3390/app15137203

Copyright: © 2025 by the authors. Licensee MDPI, Basel, Switzerland. This article is an open access article distributed under the terms and conditions of the Creative Commons Attribution (CC BY) license (https://creativecommons.org/licenses/by/4.0/).

1. Introduction

The widespread and extensive use of pharmaceutical products, while being beneficial, has also led to environmental problems worldwide and has been detected in soil, municipal sewage systems, and surface water [1]. Pharmaceuticals include a wide range of compounds such as anti-inflammatory drugs, antiretrovirals (ARVs), vaccines, steroids, painkillers, etc. [2].

Ibuprofen (IBU), 2-[4-(2-methylpropyl) phynyl] propanoic acid ($C_{13}H_{18}O_2$), is a well-known commonly used drug, with an annual consumption of more than 2 million tons. It is non-steroidal and anti-inflammatory and is usually prescribed to relieve inflammation, osteoarthritis, and rheumatoid arthritis. It is also an analgesic and mixed with other medicines to relieve fever and pain [3,4]. IBU cannot be fully metabolised in the human digestive system, and its derivatives are released from the human body through natural processes such as urination and defecation and eventually leached into the water. Prolonged intake of water containing IBU or its derivatives leads to bioaccumulation and has toxic effects on the environment, human health, and aquatic organisms [5]. Several studies have reported that the concentration of IBU is increasing in rivers and wastewater treatment plants in many countries, posing serious health and environmental risks. IBU originates from the wastewater of pharmaceutical product manufacturers, hospital effluents, the

improper disposal of expired medications, the excreta of patients taking medication, and animal husbandry [6].

The adverse effects of IBU necessitate its removal from the environment and water. Several treatment methods, including precipitation, coagulation, ion exchange, filtration, advanced oxidation [7], etc., were developed to remove pollutants from aqueous solutions. Adsorption is one of the favoured methods because it is inexpensive and effective, does not use harmful chemicals, and produces no sludge [8]. The versatility of adsorption is demonstrated by the possibility of using different materials, such as activated carbon [9], agricultural waste, zeolites [10], etc., as adsorbents.

Agricultural waste materials are economical and abundant in nature. These include pomegranate peels, papaya seeds, coconut shells and spend green tea [11], fennel seeds, hemp seeds, twigs and roots, avocado seeds, paper waste, black cumin seeds, etc. These natural materials have active sites such as oxygen-rich functional groups on their surface that can effectively bind pollutants and a porous surface that can trap pollutant molecules in water [12–17].

Rose geranium is a bushy, evergreen plant that is native to South Africa and is also found in many countries worldwide. Its unique essential oil, contained in the leaves, flowers, and stems of the plant, contains compounds such as geranial, linalool, etc [11]. The oil is highly commercialised and used in the food industry for flavouring and preservation, the pharmaceutical industry for its antibacterial and antifungal properties, and the perfume industry. After the oil is extracted from the plants, tons of waste are produced, which usually end up in the environment without any alternative use. To the best of our ability, we located a single document that reports on the use of carbon from rose geranium leaves activated by phosphoric acid (H_3PO_4) for the removal of ibuprofen from water. The great potential of using geranium leaves as an adsorbent in water purification provides a good basis for using other parts of geranium.

This research creates an alternative use for waste rose geranium stems by using them as adsorbent to remove IBU from water. In this study, we characterised the adsorbent and carried out the adsorption of ibuprofen by varying influential parameters such as initial concentration, pH of the solution, temperature of the system, and contact time.

2. Materials and Preparation

2.1. Materials

The stems of *Pelargonium graveolens* were obtained from Sebokeng, Gauteng, South Africa. Ibuprofen ($C_{13}H_{18}O_2$) $\geq$ 98%, hydrochloric acid (HCl) $\geq$ 37%, potassium nitrate (KNO_3) $\geq$ 99%, ethanol (C_2H_5OH) $\geq$ 99.5%, and sodium hydroxide (NaOH) $\geq$ 98% were purchased from Sigma Aldrich (Johannesburg, South Africa).

2.2. Experiments

2.2.1. Preparation of Pelargonium Graveolens

The stems of *Pelargonium graveolens* were ground to powder using a heavy-duty grinder. Exactly 10 g of material was transferred to a 500 mL beaker containing distilled water to remove dirt. Thereafter, the material was dried in an oven at 45 °C for 12 h. A mesh sieve was used to collect particles of 500 µm, and the material was labelled SPG.

2.2.2. Preparation of Stock Solution and Working Standards

Ibuprofen stock solution (125 mg/L) was prepared by dissolving the salt in a mixture of ethanol/water in a 1 L volumetric flask. The stock solution was diluted to prepare working standards of 25, 50, 75, 100, and 125 mg/L in 200 mL volumetric flasks.

2.2.3. Adsorption Experiments

The adsorption experiments used a mass of 0.2 g of the adsorbent (SPG) and a volume of 20 mL of IBU solutions at a temperature 35 °C, agitated at 200 rpm for 105 min unless otherwise stated. The initial concentration effect was tested using IBU working standard solutions of 25, 50, 75, 100, and 125 mg/L. The contact time effect was investigated between 1 and 105 min using an IBU solution of 125 mg/L. The temperature effect was investigated between 25, 30, 35, 40 and 45 °C using the IBU standard of 125 mg/L for 105 min. The effect of pH was examined at pH 1, 3, 5, 7, and 9 with an IBU solution of 125 mg/L. The adsorption experiments were carried out in triplicate to ensure repeatability.

2.2.4. Point Zero Charge

The experiment was carried out by transferring 50 mL of 0.01 M KNO_3 solution into ten capped bottles. The initial pH of the solutions in the bottles was adjusted to different pH values between 1 and 10. Exactly 0.1 g of SPG material was added into all the bottles and stirred for 48 h. Thereafter, the final pH was measured. The ΔpH was determined by subtracting the final pH from the initial pH. The obtained ΔpH values were plotted against initial pH values and the intercept point was determined as $pH_{(PZC)}$.

2.2.5. Reusability

The reusability of SPG was determined by reusing the adsorbent loaded with IBU. The adsorbent was added to 20 mL of a 0.1 M HCl solution and shaken at 200 rpm for 30 min to desorb IBU. The SPG was then rinsed with ultrapure water for 30 min.

2.3. Analytical Methods

SEM coupled with EDX (Thermo Fisher, Waltham, MA, USA) was used to characterise the surface morphology and the elemental constituents of the adsorbent. FTIR (Perkin Elmer, Waltham, MA, USA) was used to identify the functional groups on the surface of the adsorbent. The TGA 4000 thermogravimetric analyser (Thermo Fisher) was used to determine the thermal stability of the adsorbent under nitrogen atmosphere between 30 and 900 °C. Nitrogen adsorption–desorption studies were investigated using the Micromeritics Tristar II 3020, after degassing the sample at 40 °C. A UV-visible spectrometer (Thermo Fisher Scientific) was used to confirm the concentration of IBU in the solution before and after adsorption, with the wavelength set at 223 nm.

2.4. Data Management

The adsorption capacity, q_e (mg/g) of IBU by SPG was calculated using Equation (1).

$$q_e = \frac{(C_o - C_e)\, V}{W} \quad (1)$$

Other equations used are shown in the Supplementary Materials.

3. Characterisation

3.1. FTIR Analysis

The FTIR spectrum for SPG shown in Figure 1 indicates several characteristic peaks. The peaks are located at wavenumbers 3296 and 2919 and 2834, 1728, and 1604 and between 1065 and 1027 cm^{-1}. The broad peak at 3296 cm^{-1} corresponds to (−OH) in lignocellulose, peaks at 2919 and 2834 cm^{-1} are attributed to aliphatic (−CH) groups; other sharp peaks at 1728 and 1604 cm^{-1} correspond to carbonyl (−C=O) and amine (−NH), respectively, while the peak between 1065 and 1027 cm^{-1} is assigned to the cellulose group (−COC). Similar

peaks were observed for rose geranium leaves. It is expected that the oxygen-containing groups influence the adsorption process.

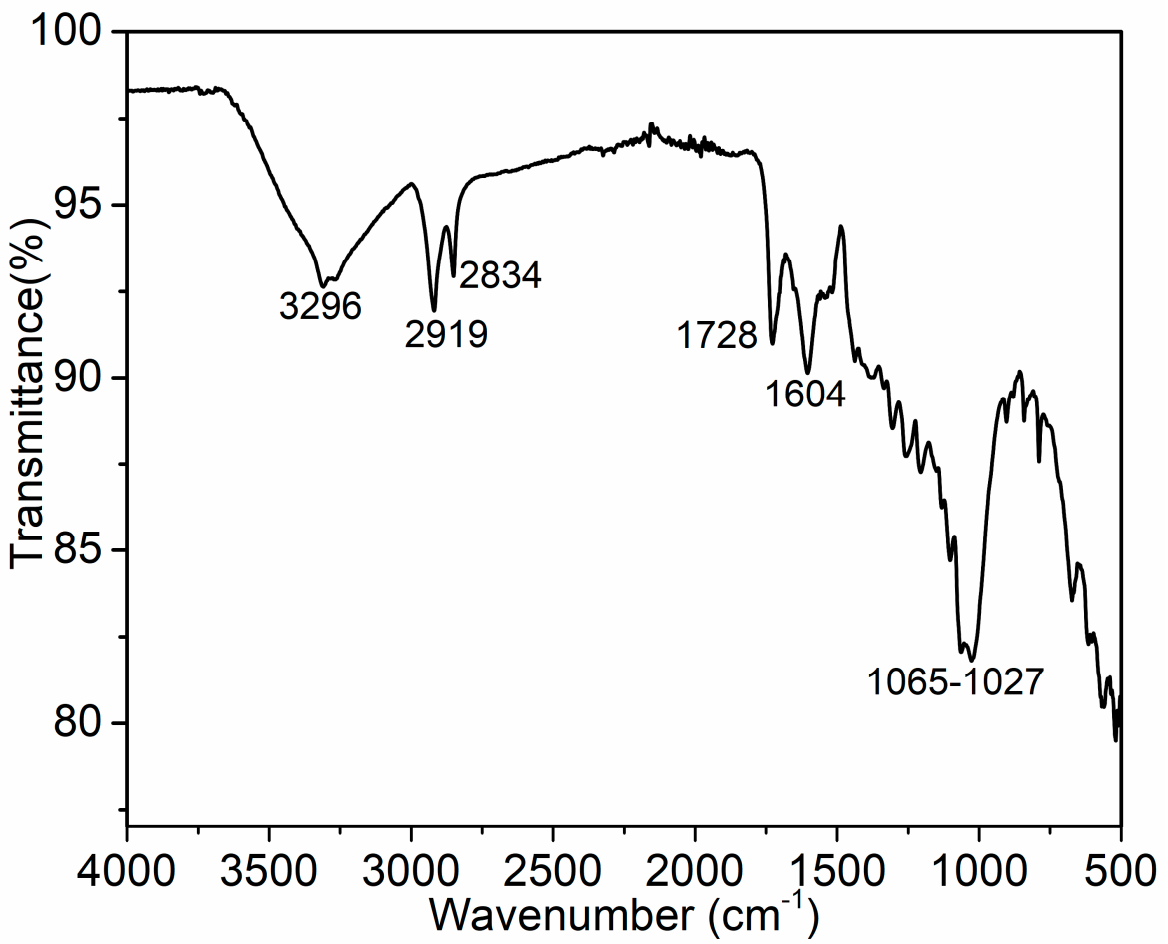

Figure 1. FTIR spectrum of SPG.

3.2. SEM-EDX Analysis

The SEM images of SPG depicted in Figure 2a–e show two-dimensional particles that are amorphous without any uniform sizes and shapes. The particles have a rough surface texture with wrinkles (Figure 2b,c) and some have openings and pores (Figure 2d). It is assumed that these properties play an important role in adsorption. A similar observation was made when rose geranium leaves were carbonised. EDX analysis (Table 1) showed C and O as major elements with trace amounts of heteroatoms.

Table 1. EDX analysis for SPG.

EDX (Weight%)						
C	**O**	**Mg**	**Ca**	**S**	**Cl**	**K**
61.22	37.83	0.11	0.28	0.08	0.14	0.33

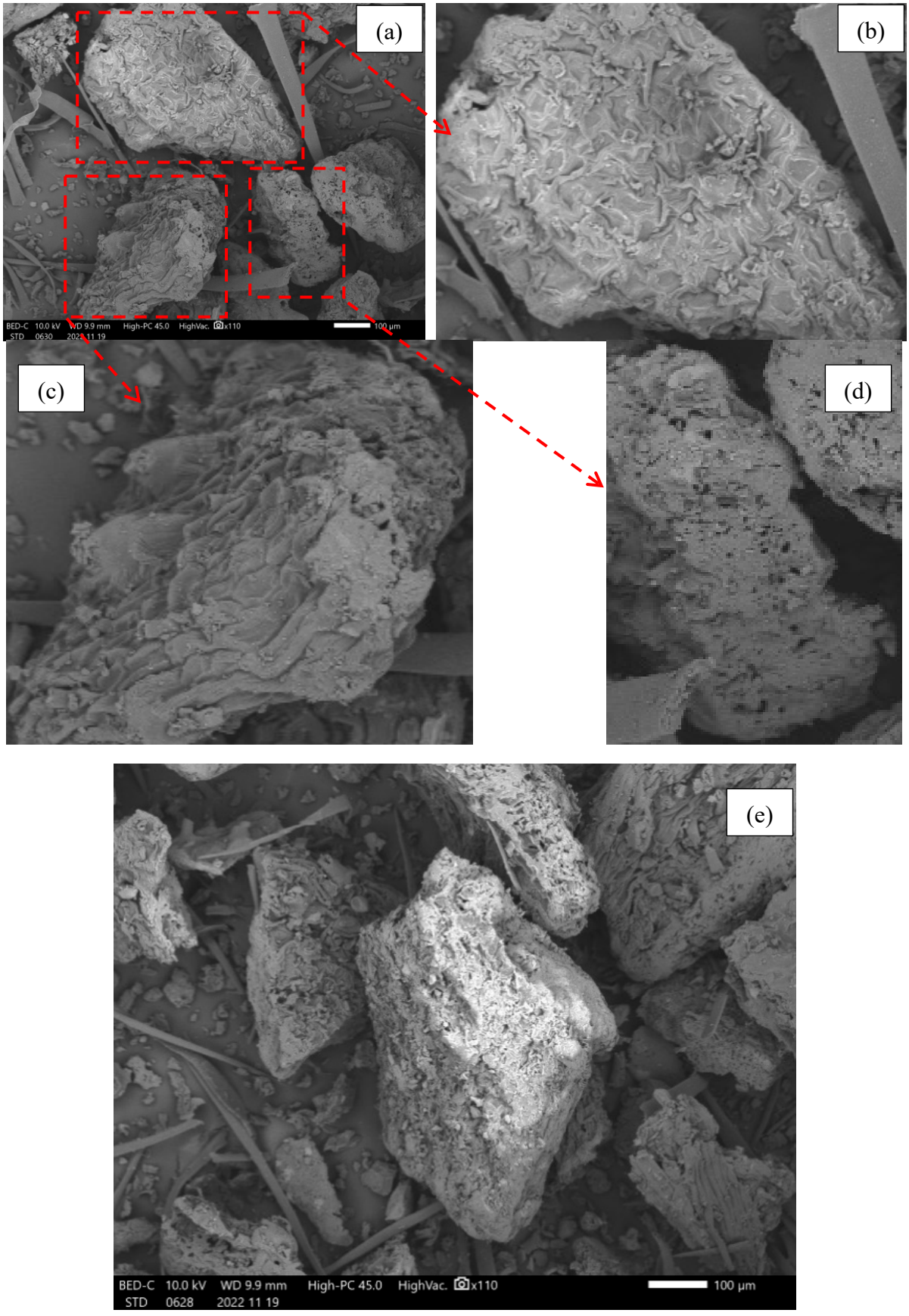

Figure 2. SEM images (**a**–**e**) for SPG.

3.3. Thermogravimetric Analysis

The thermal stability of SPG was monitored and the profile shown in Figure 3 shows two stages of decomposition. The first decomposition between 32 and 180 °C is minimal and is due to the loss of moisture; a mass loss of about 7% was observed [18]. The second decomposition between 180 and 510 °C is more significant and is due to the degradation of lignocellulosic material, with a mass loss of 52% observed [19]. Thereafter, between 510 and 900 °C, pyrolysis of the residues occurred and about 35% weight loss indicates that SPG is thermally stable.

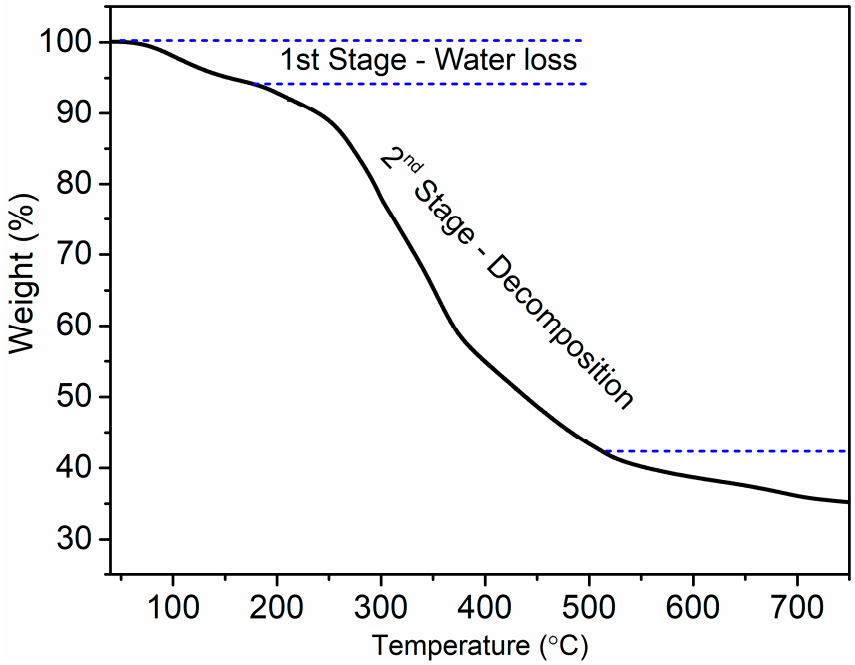

Figure 3. TGA profile of SPG.

3.4. BET Analysis

The surface area and average pore diameter of the adsorbent were measured by BET spectroscopy (Figure 4a,b). The analysis for N_2 adsorption and desorption BET surface area for SPG is 3.527 m^2/g (Figure 4a), and the adsorbent has mesopores with an average pore diameter of 3.796 nm (Figure 4b).

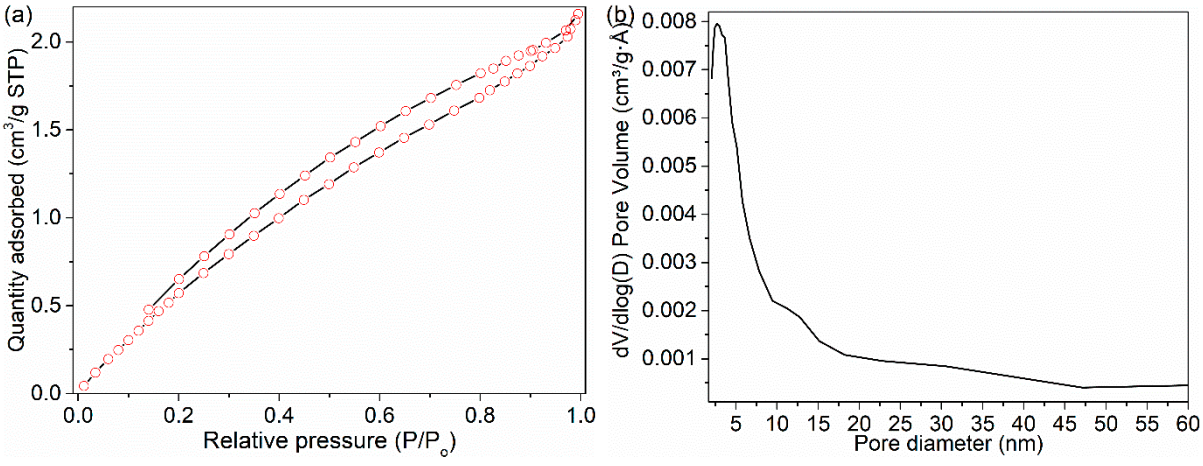

Figure 4. BET analysis (**a**) surface area and (**b**) average pore diameter.

3.5. Adsorption Results

3.5.1. Time Effect of SPG and Kinetic Models

The adsorption of IBU was studied at intervals of 1–105 min to understand the rate of uptake (Figure 5). It was found that the adsorption rate in the initial phase between 1 and 45 min was rapid. This is due to the interaction between IBU and the active sites such as functional groups containing oxygen, rough texture, pores, and voids on the surface of SPG [20]. Subsequently, a slow adsorption rate occurred, resulting in little to no adsorption in time intervals of 65–105 min. This is attributed to the progressive saturation of the active sites, which limits the adsorption rate and leads to equilibrium [21].

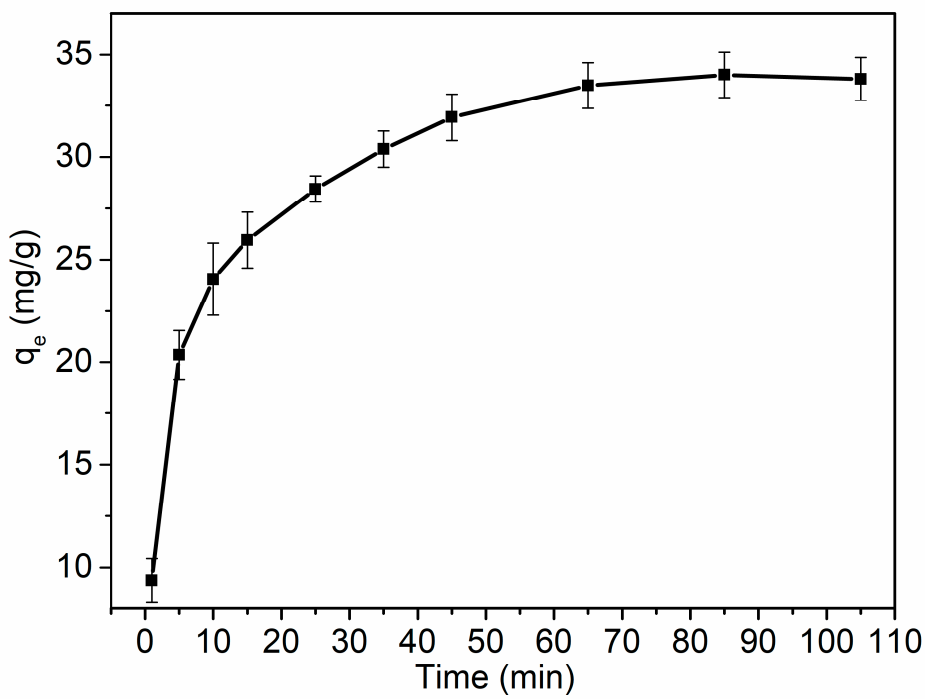

Figure 5. Time effect on SPG for ibuprofen.

The data on the time effect were recorded and fitted to two known kinetic models, which are listed in Table 2. This was to test the model best suited to the data. Pseudo-first-order (PFO) and pseudo-second-order (PSO) kinetic models are based on physisorption and chemisorption, respectively [22]. The selection criterion is based on the comparison of the correlation coefficient (r^2), which is closest to 1. The review shows that PFO has an r^2 value closer to 1. This indicates that the data fit PFO rather than PSO. The uptake of IBU on SPG is mainly through physisorption driven by weak van der Waals forces [23]. The model also predicted a Q_o value closer to the experimental q_e. The intra-particle diffusion (IPD) kinetic model-estimated pore adsorption (EPA) was 23.44%, and the estimated surface adsorption (ESA) was 76.56%.

Table 2. Kinetic models of SPG.

PFO		PSO		IPD	
Q_o (mg/g)	31.66	q_e (mg/g)	27.23	C (mg/g)	27.23
b (L/mg)	0.102	1/n	2.56	K_i (g/g·min$^{1/2}$)	1.43
R^2	0.9918	k_f	1.007	R^2	0.8187
		R^2	0.8475	EPA (%)	23.44
				ESA (%)	76.56

Experimental (q_e) (mg/g) 34.88.

3.5.2. Temperature Effect and Thermodynamics of SPG

The removal of IBU was studied at different temperatures to evaluate the effect on uptake. The temperature effect was studied between 25 and 45 °C, and the graph is shown in Figure 6. The removal of IBU increased significantly between 25 and 35 °C, showing that uptake favours an endothermic system [24]. However, the removal decreased slightly between 35 and 45 °C, indicating an exothermic nature and that a higher temperature was unfavourable for uptake. This is due to the IBU molecules gaining kinetic energy in the solution, resulting in higher mobility and reduced uptake [25].

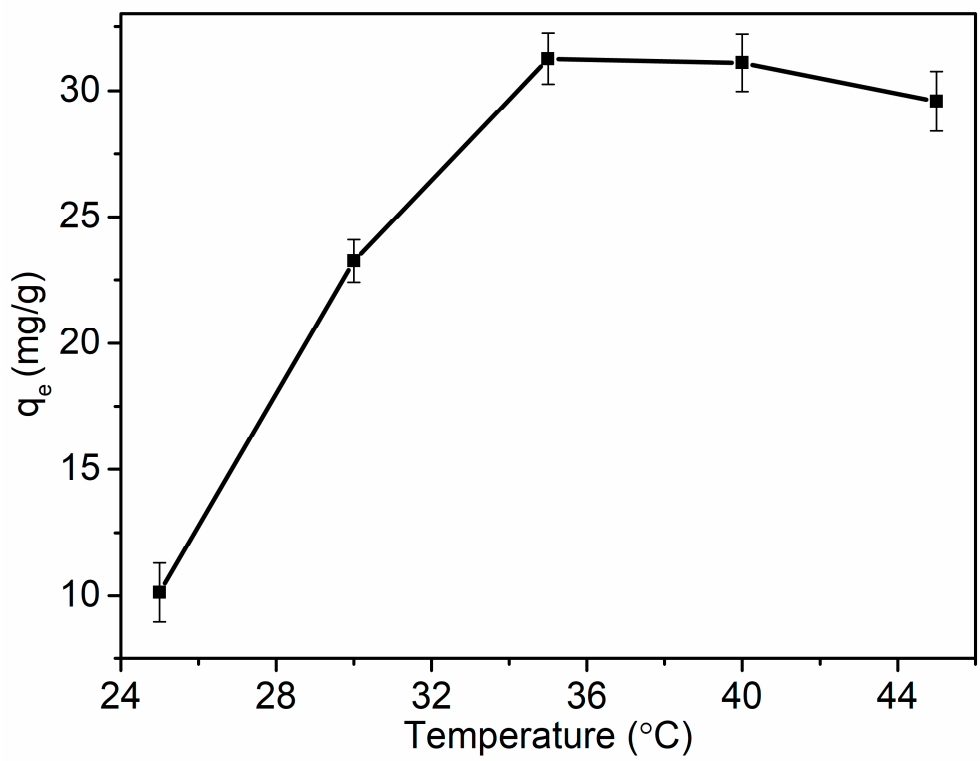

Figure 6. Temperature effect on SPG for ibuprofen.

The temperature effect data were used to determine the thermodynamic parameters, which are listed in Table 3. The values for ΔH^o were between 25 and 35 °C endothermic and between 35 and 45 °C exothermic. When the value of ΔH^o is in the range of 0 and −20 KJ/mol, the reaction is physisorption, while ΔH^o between −80 and −400 KJ/mol means chemisorption [26]. The ΔH^o value shows that the adsorption of IBU on SPG was controlled by physisorption due to weak van der Waals forces. The obtained values of ΔG^o are negative, indicating that the uptake of IBU was spontaneous. The value of ΔS^o is positive, indicating that there was increased freedom when equilibrium was reached.

Table 3. Thermodynamic parameters of SPG.

ΔH^o (KJ/mol)	ΔS^o (KJ/mol)	Temperature (K)	ΔG^o (KJ/mol)
-1×10^{-3}	3×10^{-3}	25	−4.88
		30	−2.87
		35	−2.10
		40	−1.97
		45	−1.89

3.5.3. Concentration Effect and Isotherm Models for SPG

The concentration effect was investigated using working standards with an initial concentration between 25 and 125 mg/L (Figure 7). The trends for IBU adsorption show that adsorption capacity increases when the initial concentration of the working standards is increased. The increase was recorded for standards between 25 and 100 mg/L. Thereafter, for standards with a concentration between 100 and 125 mg/L, no significant adsorption was recorded. This indicates that the active sites and binding points on SPG were saturated [27]. The mass transfer was limited and resulted in reduced uptake for the working standard of 125 mg/L.

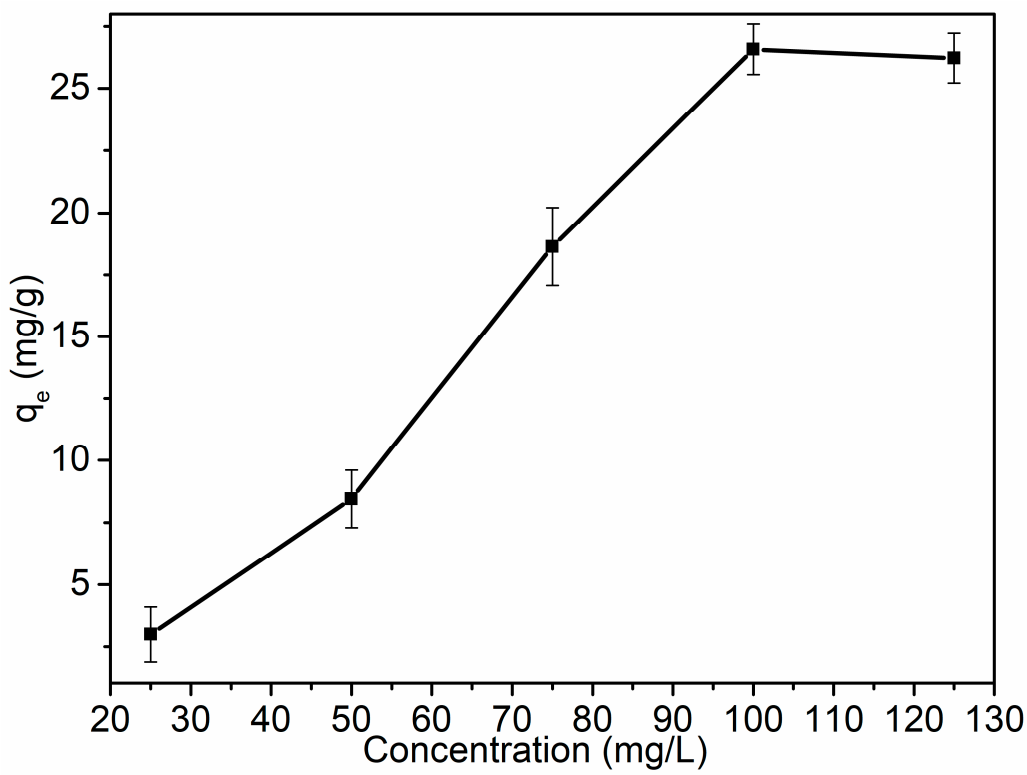

Figure 7. Concentration effect on SPG for ibuprofen.

The equilibrium data were fitted to the isotherm models (Table 4) to investigate the appropriate model and determine the interaction between SPG and IBU. Langmuir and Freundlich models are based on single-layer and multilayer adsorption, respectively [28]. The selection of the appropriate model is based on the comparison of the (r^2) values closest to 1. Table 4 shows that Langmuir has an r^2 value closer to 1 than the Freundlich model, indicating that the equilibrium data follow Langmuir's isotherm model. This suggests that uptake occurs on the surface of SPG, with the active sites having the same affinity for IBU [29]. The statistical error analysis was calculated to evaluate the most effective model by determining Marquart's percentage standard deviation (MPSD) and root mean square error (RMSE). The values obtained for MPSD and RMSE are 2.32 and 3.68 for Langmuir, respectively. The Freundlich model showed greater errors with an MPSD value of 17.69 and an RMSE value of 22.57. The Langmuir model showed lower error values for the adsorption of ibuprofen on SPG.

Table 4. Isotherm models of SPG.

Langmuir		Freundlich	
Q_o (mg/g)	24.91	q_e (mg/g)	2.4
b (L/mg)	0.0367	1/n	3.12
R^2	0.9957	k_f	0.053
MPSD	2.32	R^2	0.8836
RMSE	3.68	MPSD	17.69
Experimental q_e (mg/g) 26.58		RMSE	22.57

3.5.4. pH Effect of SPG

The influence of the pH value of the IBU solution was measured in the pH range of 1–9 (Figure 8). The trend shows that the removal was low at solution pH 1 and 3. Under these conditions, the pH of the solution is lower than the pK_a of IBU, resulting in IBU being present as a neutral molecule [30]. This restricted uptake and limited the interaction between SPG and IBU. However, the removal improved when the pH of the solution was adjusted to 5, which was due to the coexistence of IBU as a neutral and anionic species [5]. This improved electrostatic interaction and increased removal. The highest removal was observed under pH 7, with an uptake of 29.71 mg/g. This is because under these conditions, IBU molecule uptake was enhanced by electrostatic attraction between IBU present in the solution as an anion and SPG [31]. However, at pH 9, the capacity slightly decreased to 29.30 mg/g, due to enhanced electrostatic repulsion between negatively charged IBU molecules and the adsorbent surface. Under these conditions, adsorption could have occurred through other mechanisms.

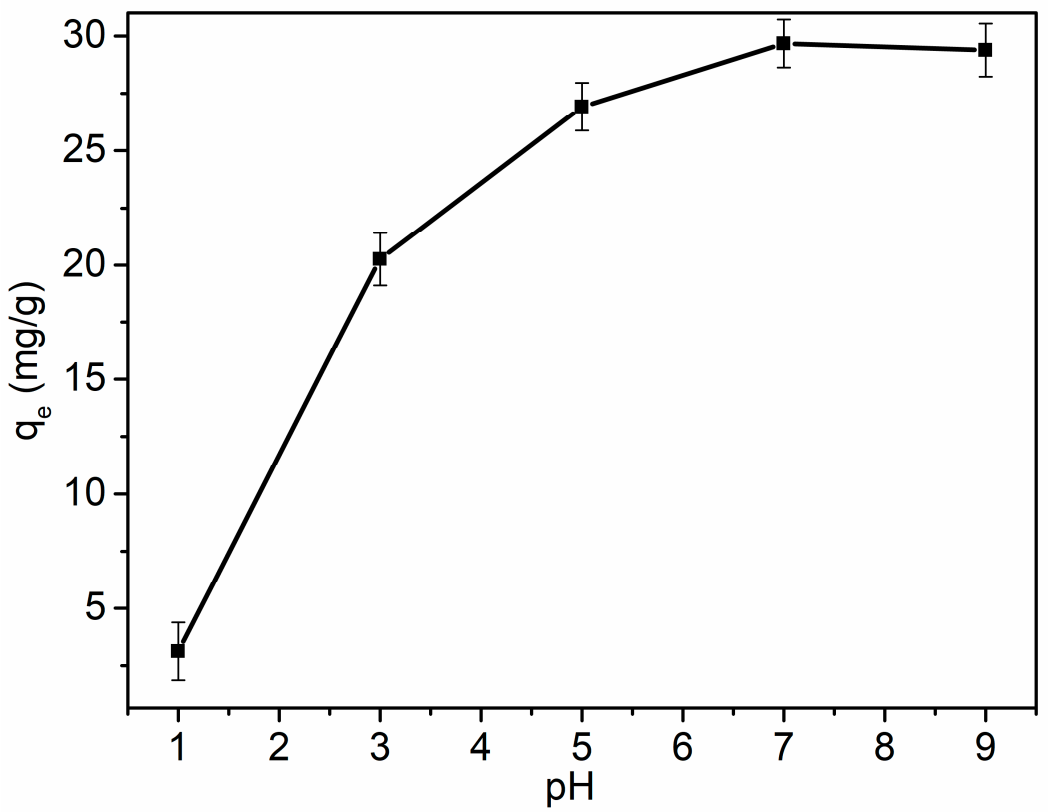

Figure 8. pH effect on SPG for ibuprofen.

3.5.5. $pH_{(PZC)}$ of SPG

To determine the neutral state of SPG. $pH_{(PZC)}$ was determined by plotting ΔpH against the initial pH, as shown in Figure 9. It was found that the $pH_{(PZC)}$ value for SPG is 4.4. At this value, the material is not charged or neutral. This indicates that SPG acquires a positive charge at initial pH values below $pH_{(PZC)}$ (i.e., from 1 to 4.3). However, at initial pH values above $pH_{(PZC)}$ for SPG 4.5 and above, the SPG acquired a negative charge.

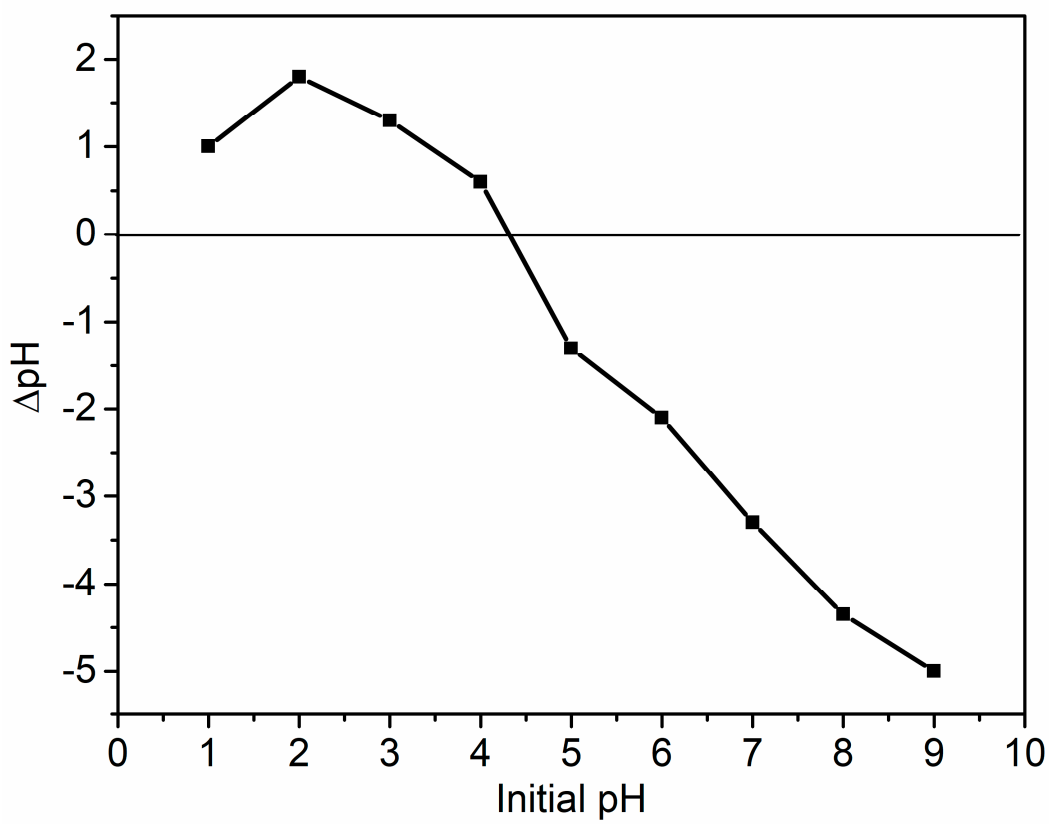

Figure 9. pH at point zero charge on SPG for ibuprofen.

3.5.6. Reusability Study of SPG

The reusability of the material was determined by the regeneration and reuse of SPG in up to four cycles (Figure 10). It was observed that the material had the highest percentage uptake during initial use—this is attributed to the abundance of active sites and binding points on SPG. Thereafter, the material gradually lost its adsorption capacity after each cycle, which is due to the inability of SPG to desorb and release IBU, resulting in a lower percentage of adsorption and capacity uptake.

3.5.7. Comparative Study

The adsorption capacity achieved for SPG was compared to similar adsorbents, as shown in Table 5. SPG waste is inexpensive but performs better than other adsorbents, demonstrating its potential for water treatment. SPG has a rough surface texture with voids and pores on the surface and abundant active sites, which may have contributed to the high adsorption capacity.

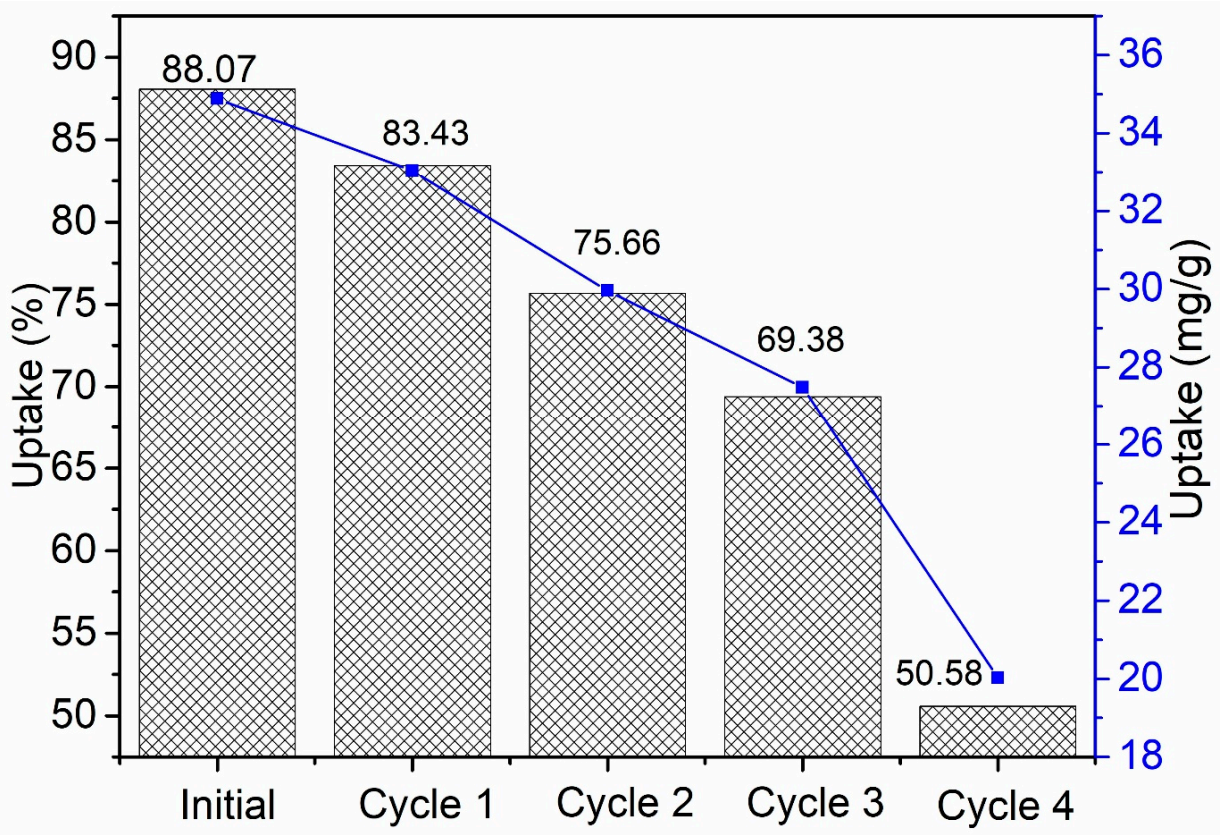

Figure 10. Reusability study on SPG for ibuprofen.

Table 5. Comparison study of the removal of IBU using similar materials.

Biosorbent	q_e (mg/g)	Reference
Carbon/magnetite NP	51.00	[32]
Blend carbon	45.58	[5]
Pomegranate husk/Fe(II)–Fe(III) NP	39.80	
Stem of rose geranium	34.88	This study
Biochar from walnut shells	30.10	[33]
Hemp seeds-MnO/CuO	26.50	[4]
Sugarcane waste	13.51	[34]
Carbon from olive seeds	9.090	[35]
Mugwort leaves	6.800	[36]

4. Conclusions

In this study, the stem of rose geranium was used as an adsorbent for ibuprofen. The material was characterised by SEM-EDX, FTIR, TGA, and BET. The SEM images showed that the morphology of the SPG exhibited a rough surface texture with voids and pores. The FTIR spectrum showed the presence of groups such as −OH, −C=O, −COC, and −NH on the surface of the adsorbent. The chemical and physical properties of SPG played an important role in the removal of IBU. IBU was found to be present as a neutral molecule in the solution at pH 1 and 3, limiting the interaction and resulting in low uptake. At pH 5, IBU was slightly ionised and coexisted as a neutral and anionic species. Under alkaline conditions at pH 7, IBU was completely ionised and existed as an anion, which improved removal. The trend of IBU adsorption showed that the adsorption capacity increases when the initial concentration of working standards is increased. The data for the time effect showed that the adsorption rate was fast in the initial phase between 1 and 45 min. This was followed by a slow adsorption rate leading to little to no adsorption in time intervals

between 65 and 105 min. The data corresponded to the Langmuir and PFO models. The ΔH^o value shows that the adsorption of IBU on SPG was controlled by physisorption due to weak van der Waals forces. The obtained values of ΔG^o are negative, indicating that the uptake of IBU was spontaneous. The reusability of SPG showed good uptake for three cycles with an efficiency of more than 65%; thereafter, the adsorbent showed limited efficiency. Overall, the results for low-cost SPG show great potential and feasibility for water treatment. Future research for SPG includes carbonization at different temperatures using various techniques such as furnace, microwave, and hydrothermal energy, followed by carbon activation with acids and bases. Such materials should also be investigated for the adsorption of other emerging pollutants.

Supplementary Materials: The following supporting information can be downloaded at: https://www.mdpi.com/article/10.3390/app15137203/s1.

Author Contributions: Conceptualization, N.D.S. and P.M.T.; methodology, P.M.T.; validation, N.D.S. and P.M.T.; formal analysis, P.M.T.; investigation, P.M.T.; resources, P.M.T.; data curation, P.M.T.; writing—original draft preparation, N.D.S. and P.M.T.; writing—review and editing, N.D.S.; visualization, N.D.S. All authors have read and agreed to the published version of the manuscript.

Funding: Vaal University of Technology, Vanderbijlpark, South Africa, funded this work.

Institutional Review Board Statement: Not applicable.

Informed Consent Statement: Not applicable.

Data Availability Statement: The data presented in this study are available on request from the corresponding author. The data are not publicly available due to privacy.

Conflicts of Interest: The authors declare no conflicts of interest.

References

1. Munzhelele, E.P.; Mudzielwana, R.; Ayinde, W.B.; Gitari, W.M. Bodies of South Africa: A Review of Sources, Pathways, Occurrence, Effects, and Geographical Distribution. *Water* **2024**, *16*, 796. [CrossRef]
2. Sigonya, S.; Mokhotu, T.H.; Mokhena, T.C.; Makhanya, T.R. Mitigation of Non-Steroidal Anti-Inflammatory and Antiretroviral Drugs as Environmental Pollutants by Adsorption Using Nanomaterials as Viable Solution—A Critical Review. *Appl. Sci.* **2023**, *13*, 772. [CrossRef]
3. Yang, Z.; Zhang, H.; Zheng, Y.; Zhang, Y.; Cui, Y. Direct activation of petroleum pitch-based mesoporous carbon for phenol adsorption. *Colloids Surf. A Physicochem. Eng. Asp.* **2024**, *702*, 135020. [CrossRef]
4. Zhang, T.; Zhang, X.; Li, H. Kinetics and equilibrium study of phenol adsorption by activated carbon derived from pig blood. *Carbon Trends* **2023**, *12*, 100281. [CrossRef]
5. Osman, A.L.; Ayati, A.; Farghali, M.; Krivosshapkin, P.; Tanhaei, B.; Karimi-Maleh, H.; Krivoshapkina, E.; Taheri, P.; Tracey, C.; Al-Fatesh, A.; et al. Advanced adsorbents for ibuprofen removal from aquatic environments: A review. *Environ. Chem. Letter.* **2024**, *22*, 373–418. [CrossRef]
6. Samal, K.; Mahapatra, S.; Ali, M.H. Pharmaceutical wastewater as emerging contaminants (EC): Treatment technologies, impact on environment and human health. *Energy Nexus* **2022**, *6*, 100076. [CrossRef]
7. Rogowska, J.; Zimmermann, A. Household Pharmaceutical Waste Disposal as a Global Problem—A Review. *Int. J. Environ. Res. Public Health* **2022**, *19*, 15798. [CrossRef]
8. Satyam, S.; Patra, S. Innovations and challenges in adsorption-based wastewater remediation: A comprehensive review. *Heliyon* **2024**, *10*, 29573. [CrossRef]
9. Gokce, Y.; Aktas, Z. Nitric acid modification of activated carbon produced from waste tea and adsorption of methylene blue and phenol. *Appl. Surf. Sci.* **2014**, *313*, 352–359. [CrossRef]
10. Velarde, L.; Nabavi, M.S.; Escalera, E.; Antti, M.L.; Akhtar, F. Adsorption of heavy metals on natural zeolites: A review. *Chemosphere* **2023**, *328*, 138508. [CrossRef]

11. Duwiejuah, A.B.; Adjei, E.F. Alhassan EH. Adsorption of toxic metals from greywater using coconut husk biochar and spent green tea. *Heliyon* **2024**, *10*, 38189. [CrossRef] [PubMed]
12. Fayoumi, L.; Khalil, M.; Ghareeb, D.; Chokr, A.; Bouaziz, M.; El-Dakdouki, M.H. Phytochemical constituents and therapeutic effects of the essential oil of rose geranium (*Pelargonium* hybrid) cultivated in Lebanon. *S. Afr. J. Botany* **2022**, *147*, 894–902. [CrossRef]
13. Thillainayagam, B.P.; Saravanan, P.; Ravindiran, G.; Josephraj, J. Continuous sorption of methylene blue dye from aqueous solution using effective microorganisms-based water hyacinth waste compost in a packed column. *Biomass Convers. Biorefinery* **2023**, *13*, 1189–1198. [CrossRef]
14. Boukhatem, N.M.; Kameli, A.; Ferhat, M.A.; Saidi, F.; Mekarnia, M. Rose geranium essential oil as a source of new and safe anti-inflammatory drugs. *Libyan J. Med.* **2013**, *7*, 22520. [CrossRef]
15. Carmen, G.; Hnncu, G. Antimicrobial and Antifungal Activity of *Pelargonium roseum* Essential Oils. *Adv. Pharm. Bull.* **2014**, *31*, 511–514.
16. Jia, Z.; Li, Z.; Ni, T.; Li, S. Adsorption of low-cost absorption materials based on biomass (*Cortaderia selloana* flower spikes) for dye removal: Kinetics, isotherms and thermodynamic studies. *J. Mol. Liq.* **2017**, *229*, 285–292. [CrossRef]
17. Mane, P.V.; Rego, R.M.; Yap, P.L.; Losic, D.; Kurkuri, M.D. Unveiling cutting-edge advances in high surface area porous materials for the efficient removal of toxic metal ions from water. *Prog. Mat. Sci.* **2024**, *146*, 101314. [CrossRef]
18. Shen, D.K.; Gu, S. The mechanism for thermal decomposition of cellulose and its main products. *Bioresour. Technol.* **2009**, *100*, 6496–6504. [CrossRef]
19. Ornaghi, H.L.; Ornaghi, F.G.; Neves, R.M.; Monticeli, F.; Bianchi, O. Mechanisms involved in thermal degradation of lignocellulosic fibers: A survey based on chemical composition. *Cellulose* **2020**, *27*, 4949–4961. [CrossRef]
20. Adebayo, G.B.; Jamiu, W.; Okoro, H.K.; Okeola, F.O.; Adesina, A.K.; Feyisetan, O.A. Kinetics, Thermodynamics and Isothermal Modelling of Liquid Phase Adsorption of Methylene Blue onto Moringa Pod Husk Activated Carbon. *S. Afr. J. Chem.* **2019**, *72*, 263–273. [CrossRef]
21. Elkhaleefa, A.; Ali, I.H.; Brima, E.I.; Shigidi, I.; Elhag, A.B.; Karama, B. Evaluation of the Adsorption Efficiency on the Removal of Lead(II) Ions from Aqueous Solutions Using Azadirachta indica Leaves as an Adsorbent. *Processes* **2021**, *9*, 559. [CrossRef]
22. Guo, X.; Wang, J. A general kinetic model for adsorption: Theoretical analysis and modelling. *J. Mol. Liq.* **2019**, *288*, 111100. [CrossRef]
23. Brandani, S. Kinetics of liquid phase batch adsorption experiments. *Adsorption* **2021**, *27*, 353–368. [CrossRef]
24. Oba, S.N.; Ighalo, J.O.; Aniagor, C.O.; Igwegbe, C.A. Removal of ibuprofen from aqueous media by adsorption: A comprehensive review. *Sci. Total Environ.* **2021**, *780*, 146608. [CrossRef]
25. Mondal, S.; Aikat, K.; Halder, G. Biosorptive uptake of ibuprofen by chemically modified *Parthenium hysterophorus* derived biochar: Equilibrium, kinetics, thermodynamics and modelling. *Ecol. Eng.* **2016**, *92*, 158–172. [CrossRef]
26. Sutherland, C. Adsorption of cephalexin: A decade of progress in adsorbent development and mechanistic insights. *Desalin. Water Treat.* **2024**, *318*, 100357. [CrossRef]
27. Kamdod, A.S.; Kumar, M.V.P. Adsorption of methylene blue, methyl orange, and crystal violet on microporous coconut shell activated carbon and its composite with chitosan: Isotherms and kinetics. *J. Polym. Environ.* **2022**, *30*, 5274–5289. [CrossRef]
28. Mahajan, T.; Paikaray, S.; Mahajan, P. Applicability of the equilibrium adsorption isotherms and the statistical tools on to them: A case study for the adsorption of fluoride onto Mg-Fe-CO_3 LDH. *J. Phys. Conf. Ser.* **2023**, *2603*, 012056. [CrossRef]
29. Cozmuta, L.M.; Cozmuta, A.M.; Peter, A.; Nicula, C.; Nsimba, E.B.; Tutu, H. The influence of pH on the adsorption of lead by Na-clinoptilolite: Kinetic and equilibrium studies. *Water SA* **2012**, *38*, 269–278. [CrossRef]
30. Yamin, M.; Ghouri, Z.K.; Rohman, N.; Syed, J.A.; Skelton, A.; Ahmed, K. Unravelling pH/pKa influence on pH-responsive drug carriers: Insights from ibuprofen-silica interactions and comparative analysis with carbon nanotubes, sulfasalazine, and alendronate. *J. Mol. Graph. Model.* **2024**, *128*, 108720. [CrossRef]
31. Ayati, A.; Tanhaei, B.; Beiki, H.; Krivoshapkin, P.; Krivoshapkina, E.; Tracey, C. Insight into the adsorptive removal of ibuprofen using porous carbonaceous materials: A review. *Chemosphere* **2023**, *323*, 138241. [CrossRef] [PubMed]
32. Labuto, G.; Carvalho, A.P.; Mestre, A.S.; dos Santos, M.S.; Modesto, H.R.; Martins, T.D.; Lemos, S.G.; da Silva, H.G.T.; Neide, E.; Carrilho, E.N.V.M.; et al. Individual and competitive adsorption of ibuprofen and caffeine from primary sewage effluent by yeast-based activated carbon and magnetic carbon nanocomposite. *Sustain. Chem. Pharm.* **2022**, *28*, 100703. [CrossRef]
33. Patel, M.; Chaubey, A.K.; Pittman, C.U.; Mohan, D. Aqueous ibuprofen sorption by using activated walnut shell biochar: Process optimization and cost estimation. *Environ. Sci. Adv.* **2022**, *1*, 530–545. [CrossRef]
34. Chakraborty, P.; Show, S.; Banerjee, S.; Halder, G. Mechanistic insight into sorptive elimination of ibuprofen employing bidirectional activated biochar from sugarcane bagasse: Performance evaluation and cost estimation. *J. Environ. Chem. Eng.* **2018**, *6*, 5287–5300. [CrossRef]

35. Baccar, R.; Sarra, M.; Bouzid, J.; Feki, M.; Blanquez, P. Removal of pharmaceutical compounds by activated carbon prepared from agricultural by-product. *Chem. Eng. J.* **2012**, *211–212*, 310–317. [CrossRef]
36. Guedidi, H.; Reinert, L.; Leveque, J.M.; Soneda, Y.; Bellakhal, N.; Duclaux, N. The effects of the surface oxidation of activated carbon, the solution pH and the temperature on adsorption of ibuprofen. *Carbon* **2013**, *54*, 432–443. [CrossRef]

Disclaimer/Publisher's Note: The statements, opinions and data contained in all publications are solely those of the individual author(s) and contributor(s) and not of MDPI and/or the editor(s). MDPI and/or the editor(s) disclaim responsibility for any injury to people or property resulting from any ideas, methods, instructions or products referred to in the content.